

# PRESENTING A MODIFIED SPH ALGORITHM FOR NUMERICAL STUDIES OF FLUID-STRUCTURE INTERACTION PROBLEMS

*S. M. Hosseini and N. Amanifard\**

*Department of Mechanical Engineering, Faculty of Engineering  
University of Guilan, P.O.Box 3756, Rasht, Iran  
namanif@guilan.ac.ir*

\*Corresponding Author

(Received: April 2, 2007 – Accepted in Revised Form: May 31, 2007)

**Abstract** A modified Smoothed Particle Hydrodynamics (SPH) method is proposed for fluid-structure interaction (FSI) problems especially, in cases which FSI is combined with solid-rigid contacts. In current work, the modification of the utilized SPH concerns on removing the artificial viscosities and the artificial stresses (which such terms are commonly used to eliminate the effects of tensile and numerical instabilities) as well as decreasing the CPU time with achieving more accuracy and the easier programming in comparison with other methods in the similar cases. The mentioned performance of the proposed algorithm is assessed by solving a test case including deformation of an elastic plate subjected to time-dependent water pressure. The obtained results are in close agreement with other high accuracy methods and experimental results.

**Keywords** Smoothed Particles Hydrodynamics (SPH), Fluid-Structure Interaction (FSI) Models, Lagrangian Method, Solid-Rigid Contact, Deformation of an Elastic Plate

**چکیده** یک الگوریتم اصلاح شده از خا نواده روش "هیدرودینامیک ذرات متصل" (SPH) برای مسائل اندرکنش سیال و دیواره قابل انعطاف معرفی گردیده است. در این ارتباط، اصلاح روش بر حذف لزجی مجازی و تنش های مجازی استوار گردیده است: جملاتی که تاکنون در خانواده روش های (SPH) همواره برای کاهش ناپایداری های عددی به کار گرفته شده است. پیامد این امر سهولت بیشتر در به کار گیری روش (SPH) و نتیجتاً الگوریتم نویسی و کاهش زمان اجرای حل عددی است. روش یاد شده برای یک مسئله نمونه از مسائل اندر کنش سیال و دیواره برای نشان دادن قابلیت آن در حل توام جریان و محدوده الاستیک دیواره بدون هر نوع استفاده از شرط مرزی میانی به کار گرفته شده و نتایج با روش غیر اصلاح شده (SPH) و نتایج تجربی مقایسه گردیده است. مقایسه حاکی از ارتقای (SPH) صحت نتایج است.

## 1. INTRODUCTION

One of the interesting problems in many engineering applications is associated with solid boundary deformations due to the fluid flow. Both problems of viscous fluid flow and of elastic body deformation have been studied separately for many years in great detail. But there are many problems encountered in real life where an interaction between those two media is of great importance. Many tubes used in industries can have deformations due to interactions with other devices or to the degradation of the material constituting the tubes. A typical example of such a problem is the area of aero-elasticity. Another important area

where such interaction is of great interest is biomechanics. Such interaction is encountered especially when dealing with the blood circulatory system. Problems of a pulsatile flow in an elastic tube, flow through heart valves, flow in the heart chambers are some of the examples. In all these cases large deformations of a deformable solid interacting with an unsteady, often periodic, fluid flow must be dealt with [1].

Fluid-structure interaction models are increasingly used in biomedical engineering applications and some of the most challenging fluid-structure problems that can be found in the human body involve the dynamics of heart valves and blood flow simulation in arteries. The arterial

walls and heart muscles are compliant and therefore play an important role in the process of opening and closing. Altogether, the combination makes the problem extremely complex to model [2].

Different ways of modeling fluid-structure interaction (FSI) have been proposed in the past, each having its advantages and disadvantages. Arbitrary Lagrangian Eulerian (ALE) methods, as exploited by e.g. [3,4], are most commonly used for FSI problems and have the advantage to provide a strong coupling. As long as rotations, translations and/or deformations of the solid remain within certain limits, this method works well and is recommended. However, for problems in which these limits are violated, elements become ill-shaped and ALE alone does not suffice. As a solution to this problem an often-used combination is ALE with some form of remeshing. This can, however, be a difficult and time consuming task.

A more elegant way to solve the system allowing free movement of a structure through a fluid domain was proposed by Peskin [5]. He introduced a method that later became known as the immersed boundary method (IBM) where flow-induced solid body motions could be computed without adjusting the fluid grid/mesh.

A method that could cope with large translations and rotations was used by Glowinski et al. [6,7]. Using a fictitious domain method, the sedimentation of rigid particles in a fluid domain could be computed. The rigid particles are immersed on the fluid domain and are coupled to the fluid by applying constraints across the particle using a Lagrange multiplier. This way of coupling is allowed for large translations as well as rotations of particles.

A method that resembles the above mentioned methods was introduced by Baaijens [8] for slender deforming bodies. In this method a fluid mesh is considered with an immersed solid mesh, and the solid mesh and fluid mesh are coupled by a Lagrange multiplier (or local body forces) at the boundary of the solid. The elegance of this method is its simplicity and flexibility. Actual three-dimensional approximation is, up to now, very rare. The most common approach is the combination of separate solvers for fluid and solid by an outer coupling iteration.

Another class of the fluid structure interaction

modeling is the fluid–solid mixture model which at first was applied to swelling and diffusion in rubber materials [9] and the compression of cartilage [10].

Nevertheless, it should be pointed out that the majority of the numerical schemes developed until now belong to the class of the so-called Eulerian methods, i.e. finite element (FE), finite volumes (FV), finite difference (FD) schemes, which make use of a fixed underlying grid to discretise the set of partial differential equations of the fluid motion. Until the early 1990s only a few works focused on the design of meshless methods for an alternative description of the physical problem, based on a purely Lagrangian description. Namely, many of these were concentrating more on astrophysical and cosmological problems, for whose simulations the first fully Lagrangian (and completely meshless) numerical method was developed in the late 1970s. This corresponds to the famous works of Lucy [11], Monaghan and Gingold [12] who in 1977 simultaneously and independently developed smoothed particle hydrodynamics (SPH).

The method uses a purely Lagrangian approach and has been successfully employed in a wide range of problems. The SPH method is a branch of meshless methods and unlike Eulerian methods does not use a fixed grid to represent the computational domain. That is the method does not require connectivity data as needed by the finite volume and finite element methods. This gives the method a very useful feature when dealing with complex flows, exhibiting large deformations and/or free-surfaces. Instead the SPH method is a particle based method. The word "particle" does not mean a physical mass instead it refers to a region in space. Field variables are associated with these particles and at any other point in space are found by averaging, or smoothing, the particle values over the region of interest. This is fulfilled by an interpolation or weight function which is often called the interpolation kernel. It should be pointed out that SPH method was then successfully applied to the study of various fluid dynamics problems, such as free-surface incompressible flows [13], viscous flows [14-18], and elastic dynamics [19]. The first attempt to describe elastic solid deformation due to incompressible fluid flow was attempted by Carla Antoci et al. in [21].

The motivation of this work is to present a new

free artificial viscosity SPH algorithm for simulating elastic solids and the fluid-structure interaction problems. It will be shown that the new algorithm can be utilized more easily with more accurate results for the test problems.

A benchmark of fluid-structure interaction problems was solved and the results are compared to the experimental results and the results of FEM simulation. The benchmark problem is the deformation of an elastic plate subjected to time-dependent water pressure.

## 2. FUNDAMENTALS

The SPH method is based on the interpolation theory. The method allows any function to be expressed in terms of its values at a set of disordered points representing particle points using a kernel function. The kernel function refers to a weighing function and specifies the contribution of a typical field variable,  $A(r)$  at a certain position,  $r$  in space. The kernel estimate of  $A(r)$  is defined as [21]:

$$\langle A_h(r) \rangle = \int_{\text{Space}} A(r') W(r-r', h) dr' \quad (1)$$

Where the smoothing length  $h$  represents the effective width of the kernel and  $W$  is a weighting function with the following properties [22]:

$$\int_V W(r-r', h) dr' = 1 \quad \lim_{h \rightarrow 0} W(r-r', h) = \delta(r-r') \quad (2)$$

If  $A(r')$  is known only at a discrete set of  $N$  point  $r_1, r_2, \dots, r_N$  then  $A(r')$  can be approximated as follows [28]:

$$A(r') = \sum_{j=1}^N \delta(r'-r_j) A(r_j) (dV)_j \quad (3)$$

Where  $(dV)_j$  is the differential volume element around the point  $r_j$ . Combining Equation 1 and Equation 3 yields [28]:

$$\langle A_h(r) \rangle = \sum_{j=1}^N \int \delta(r'-r_j) A(r_j) (dV)_j W(r-r', h) dr' \quad (4)$$

After integration, and replacing the differential volume element  $(dV)_j$  by  $m_j/\rho_j$  one gets [28]:

$$\langle A_h(r) \rangle = \sum_{j=1}^N \frac{m_j}{\rho_j} A_j W(r-r', h) \quad (5)$$

Where the summation index  $j$  denotes a particle label and particle  $j$  carries a mass  $m_j$  at position  $r_j$ , a density  $\rho_j$  and a velocity  $v_j$ . The value of  $A$  at  $j$ -th particle is shown by  $A_j$ . The summation is over particles which lie within a circle of radius  $2h$  centered at  $r$ .

**2.1. Kernel Function** The kernel function is the most important ingredient of the SPH method. Various forms of kernels with different compact support were proposed by many researchers. Recent studies [13,15,16] indicate that stability of SPH algorithm depends strongly upon the second derivative of the kernel.

Using different kernels in the SPH method is similar to using different schemes in finite difference methods. One of the most popular kernels is based on spline functions [17]:

$$W(r, h) = \frac{\sigma}{h^v} \times \begin{cases} 1 - \frac{3}{2} s^2 + \frac{3}{4} s^3 & 0 \leq s < 1 \\ \frac{1}{4} (2-s)^3 & 1 \leq s < 2 \\ 0 & 2 \leq s \end{cases} \quad s = \frac{|r|}{h} \quad (6)$$

Where  $v$  is the number of dimensions and  $\sigma$  is normalization constant with the values:  $\frac{2}{3}, \frac{10}{7\pi}, \frac{1}{\pi}$  in one, two and three dimensions respectively. This kernel has compact support which is equal to  $2h$ , it means that interactions are exactly zero for  $r > 2h$ . The second derivatives of this kernel continues and the dominant error term in the integral interpolant  $O(h^2)$ . Higher order splines can be used, but they interact at further distances and thus require more computational time.

**2.2. Gradient and Divergence** The gradient and divergence operators need to be formulated in a SPH algorithm if simulation of the Navier-Stokes equations is to be attempted. In this work, the following commonly used forms are employed for a gradient of a scalar A and divergence of a vector u [22]:

$$\frac{1}{\rho_i} \nabla_i A = \sum_j m_j \left( \frac{A_i}{\rho_i^2} + \frac{A_j}{\rho_j^2} \right) \nabla_i W_{ij} \quad (7)$$

$$\frac{1}{\rho_i} \nabla_i \cdot u_i = \sum_j m_j \left( \frac{u_i}{\rho_i^2} + \frac{u_j}{\rho_j^2} \right) \nabla_i W_{ij} \quad (8)$$

Where  $\nabla_i W_{ij}$  is the gradient of kernel function  $W(|r_i - r_j|, h)$  with respect to  $r_i$ , the position of particle i. This choice of discretization operators ensures that an exact projection algorithm is produced.

**2.3. Laplacian Formulation** A simple way to formulate the Laplacian operator is to envisage it as a dot product of the divergence and gradient operators. This approach proved to be problematic as the resulting second derivative of the kernel which is very sensitive to particle disorder and can easily lead to pressure instability and decoupling in the computation due to the co-location of the velocity and pressure. In this paper, the following alternative approach is adopted [23]:

$$\nabla \cdot \left( \frac{1}{\rho} \nabla A \right)_i = \sum_j m_j \frac{8 A_{ij} r_{ij} \cdot \nabla_i W_{ij}}{(\rho_i + \rho_j)^2 |r_{ij}|^2 + \eta^2} \quad (9)$$

Where  $A_{ij} = A_i - A_j$ ,  $r_{ij} = r_i - r_j$  and  $\eta$  is a small number introduced to avoid a zero denominator during computations and is set to 0.1h.

### 3. GOVERNING EQUATIONS

In this paper a new algorithm for elastic

deformation modeling of solid particles is presented which doesn't utilize any artificial viscosity and artificial stress terms. The proposed algorithm for solid particle modeling is completely compatible with fluid particles and it Permits to easily follow the motion of fluid-solid interface in time without any specific treatment.?????

### 3.1. Governing Differential Equations for Fluid Particles

The governing equations for transient compressible fluid flow include the conservation of mass and momentum equations. In a Lagrangian framework these can be written as [27]:

$$\frac{1}{\rho} \frac{D\rho}{Dt} + \nabla \cdot v = 0 \quad (10)$$

$$\frac{Dv}{Dt} = g + \frac{1}{\rho} \nabla \cdot \tau - \frac{1}{\rho} \nabla P \quad (11)$$

Where  $t$  is time,  $g$  is the gravitational acceleration,  $P$  is pressure,  $v$  is the velocity vector,  $\tau$  is viscous stress tensor and  $D/Dt$  refers to the material derivative. The density  $\rho$  has been intentionally kept in the equations to be able to enforce the incompressibility of the fluid. The momentum equations include three driving force terms, i.e., body force, forces due to divergence of stress tensor and the pressure gradient. These must be handled along with the incompressibility constraint. In a SPH formulation the above system of governing equations must be solved for each particle at each time-step. The sequence with which the force terms are incorporated can be different from one algorithm to another.

### 3.2. Viscous Terms in Fluid Zone

It is known that In the Newtonian fluids,  $\tau$  in Equation 11 must be defined as below:

$$\tau = 2\mu D \quad (12)$$

$$D = \frac{1}{2} (\nabla v + \nabla v^t) \quad (13)$$

$$v = u \vec{i} + v \vec{j} \quad (14)$$

$\Rightarrow$   
 $\tau$  in the momentum equation appears as a divergence form which can be written in SPH formulation as below [28]:

$$\left(\frac{1}{\rho} \nabla \cdot \vec{\tau}\right)_i = \sum_j m_j \left( \frac{\vec{\tau}_i}{\rho_i^2} + \frac{\vec{\tau}_j}{\rho_j^2} \right) \cdot \nabla W(\vec{r}_i - \vec{r}_j, h) \quad (15)$$

**3.3. Governing Differential Equations for Elastic Solid Zone** The acceleration equations (Momentum equation) for Elastic Medium can be written as below [19]:

$$\frac{dv}{dt} = g + \frac{1}{\rho} \nabla \cdot \vec{\sigma} \quad (16)$$

In the above equations  $d/dt$  denotes a derivative following the motion,  $\sigma$  is the stress tensor and can be written as [19]:

$$\sigma^{ij} = -P\delta^{ij} + S^{ij} \quad (17)$$

By Combining Equation 16 and Equation 17 the final form of governing equations for Elastic Medium Motion includes the continuity and the acceleration equations which can be written as below

$$\frac{1}{\rho} \frac{D\rho}{Dt} + \nabla \cdot v = 0 \quad (18)$$

$$\frac{dv}{dt} = g + \frac{1}{\rho} \nabla \cdot \vec{S} - \frac{1}{\rho} \nabla P \quad (19)$$

Where  $g$  is the gravitational acceleration,  $P$  is pressure,  $\vec{S}$  is the deviatoric stress tensor and its rate of change is given by [19]:

$$\frac{dS^{ij}}{dt} = 2\mu \left( \dot{\varepsilon}^{ij} - \frac{1}{3} \delta^{ij} \dot{\varepsilon}^k_k \right) + S^{ik} \omega^{jk} + \omega^{ik} S^{kj} \quad (20)$$

Where [19]:

$$\dot{\varepsilon}^{ij} = \frac{1}{2} \left( \frac{\partial v^i}{\partial x^j} + \frac{\partial v^j}{\partial x^i} \right) \quad (21)$$

and the rotation tensor  $\omega^{ij}$  is [19]:

$$\omega^{ij} = \frac{1}{2} \left( \frac{\partial v^i}{\partial x^j} - \frac{\partial v^j}{\partial x^i} \right) \quad (22)$$

## 4. SOLUTION ALGORITHM

In this paper, a fully explicit three-step algorithm is used for both fluid and elastic solid particles which will be explained in detail.

**4.1. Solution Algorithm for Fluid Particles** In the first step of this algorithm, the momentum equation is solved in the presence of the body forces neglecting all other forces. So, an intermediate velocity is computed as

$$u^* = u_{t-\Delta t} + g_x \Delta t \quad (23)$$

$$v^* = v_{t-\Delta t} + g_y \Delta t \quad (24)$$

As said before, in the second step of fluid flow simulation the temporal velocity is employed to calculate the divergence of viscous stress tensor. Note that the divergence of viscous stress tensor is a vector  $\vec{T}$  given by:

$$\left(\frac{1}{\rho} \nabla \cdot \vec{\tau}\right)_i = \vec{T} = T_x \vec{i} + T_y \vec{j} \quad (25)$$

At the end of the second step, the particle velocity is updated according to

$$u^{**} = u^* + T_x \Delta t = u_{t-\Delta t} + g_x \Delta t + T_x \Delta t \quad (26)$$

$$v^{**} = v^* + T_y \Delta t = v_{t-\Delta t} + g_y \Delta t + T_y \Delta t \quad (27)$$

At this stage the particle moved according to temporal velocities ( $u^{**}, v^{**}$ ) and temporal position of the particle is:

$$x^* = x_{t-\Delta t} + u^{**} \Delta t \quad (28)$$

$$y^* = y_{t-\Delta t} + v^{**} \Delta t \quad (29)$$

Thus far no constraint has been imposed to satisfy the incompressibility of the fluid and it is expected that the density of some particles change during this updating. In fact, with the help of the continuity equation one can calculate the density variations of each particle as

$$\frac{D\rho_i}{Dt} = \sum_j m_j (v_i - v_j) \cdot \nabla_i W(r_{ij}, h) \quad (30)$$

Where  $\rho_i$  and  $v_i$  are the density and velocity of particle  $i$ . When two particles approach each other, their relative velocity and therefore the gradient of kernel function become negative, so  $D\rho_i/Dt$  will be positive and  $\rho_i$  will increase. Consequently, this will produce a repulsive force between the approaching particles. In a similar fashion, if two particles are repulsed from each other, an attractive force will be produced to stop this. This interaction based on the relative velocity of particles and the resulting coupling between the pressure and density will enforce incompressibility in the solution procedure.

The velocity field  $\hat{v} = (\hat{u}, \hat{v})$  which is needed to restore the density of particles to their original value is now calculated. To do this, in the third step of the algorithm, the momentum equation with the pressure gradient term as a source term is combined with the continuity Equation 10 as

$$\frac{1}{\rho_0} \frac{\rho_0 - \rho^*}{\Delta t} + \nabla \cdot (\hat{v}) = 0 \quad (31)$$

$$\hat{v} = - \left( \frac{1}{\rho^*} \nabla P \right) \Delta t \quad (32)$$

to obtain the following pressure of the Poisson equation

$$\nabla \cdot \left( \frac{1}{\rho^*} \nabla P \right) = \frac{\rho_0 - \rho^*}{\rho_0 \Delta t^2} \quad (33)$$

Equation 35 can be discretized according to Equation 9 to obtain pressure of each particle as

$$P_i = \frac{\left( \frac{\rho_0 - \rho^*}{\rho_0 \Delta t^2} + \sum_j \frac{8 m_j}{(\rho_i + \rho_j)^2} \frac{P_j \bar{r}_{ij} \cdot \nabla_i W_{ij}}{|\bar{r}_{ij}|^2 + \eta^2} \right)}{\left( \sum_j \frac{8 m_j}{(\rho_i + \rho_j)^2} \frac{\bar{r}_{ij} \cdot \nabla_i W_{ij}}{|\bar{r}_{ij}|^2 + \eta^2} \right)} \quad (34)$$

using this value for the pressure of each particle one can calculate  $\hat{v}$  according to Equation 34 and 7 as

$$\hat{v}_i = \sum_j m_j \left( \frac{P_i}{\rho_i^*} - \frac{P_j}{\rho_j^*} \right) \nabla_i W_{ij} \quad (35)$$

Finally, overall velocity of each particle at the end of the time step will be obtained as

$$u_{t+\Delta t} = u^{**} + \hat{u} \quad (36)$$

$$v_{t+\Delta t} = v^{**} + \hat{v} \quad (37)$$

And the final positions of particles are calculated using a central difference scheme in time

$$x_t = x_{t-\Delta t} + \frac{\Delta t}{2} (u_t + u_{t-\Delta t}) \quad (38)$$

$$y_t = y_{t-\Delta t} + \frac{\Delta t}{2} (v_t + v_{t-\Delta t}) \quad (39)$$

## 4.2. Solution Algorithm for Solid Particles

A comparison between governing equations of fluid and solid zones shows that only the second term in momentum equations differ from each other. So, just the second step of solution algorithm for solid particles is different from related step in fluid particles.

In fact, in the second step of fluid flow simulation in the effect of viscous term (Equation 11) is calculated in contrast of calculating the deviatoric stress for solid particles (Equation 19).

The second step of solution algorithm for solid zone starts with updating the deviatoric stress at each time step according to Equation 20 by

calculating  $\dot{\epsilon}^{ij}$  and  $\dot{\omega}^{ij}$  (Equations 21 and 22). To model an elastic-plastic material an additional yield condition is required which defines the material elastic limit and hence determines when plastic flow occurs. For the present work, the von Mises yield condition has been employed, which can be written in terms of the principal stresses,

By using the yield strength of the material in simple tension ( $\tau_Y$ ), the yield condition can be written as [25]

$$S_x^2 + S_y^2 + 2S_{xy}^2 \leq \tau_Y^2 \quad (40)$$

and it is this expression which is used here to detect the onset of plastic flow. In the numerical scheme discussed in this work, once yield is detected the material is assumed to flow plastically, resisting with a constant state of deviatoric stress; hence the term elastic-perfectly plastic.

If the above condition is satisfied then response is elastic and this is the final state of stress, otherwise the material has yielded and flow is plastic and each stress component must be rescaled to lie on the yield surface by multiplying by the rescaling factor [24]:

$$\frac{\sqrt{2/3} \tau_Y}{\sqrt{S_x^2 + S_y^2 + 2S_{xy}^2}} \quad (41)$$

Similar to the second step for the fluid zone, the divergence of deviatoric stress is utilized for calculating the temporal velocities ( $u_{**}, v_{**}$ ), then temporal position ( $x_*, y_*$ ) of particles will be calculated at the end of the second step. The third step for satisfying the incompressibility to elastic solid particles is completely similar to fluid ones.

It should be mentioned that all of the SPH algorithm for simulating solid particles utilizes an artificial viscosity term (in order to smooth out the velocity oscillations) and artificial stress (to eliminate the effects of tensile instability) but none were used in the artificial parameters in this new algorithm. In addition the pressures of solid particles are calculated by solving continuity with the third term of momentum equation (in third step of proposed algorithm) instead of using the equation.

## 5. FLUID-STRUCTURE INTERACTION MODEL

In the first attempt of the fluid-structure interaction modeling with SPH [20], some particles were defined as interface particles. The way to define the interface and its normal vector was similar to that which was proposed by [25] to define complex solid boundaries. The dynamic interface conditions were satisfied by adding some source terms to the momentum equation which is equivalent to the action-reaction principle. It was guaranteed that by imposing the force exerted by the fluid on the solid the same modulus as the force exerted by the solid, an opposite force is exerted to the fluid.

Here a different method for Fluid-structure interaction modeling is proposed. In this method it was assumed that in each time step, elastic walls play the role of rigid walls for fluid particles and only contribute in the third step of computational algorithm. In fact, when fluid particles move toward elastic particles their pressure increases and prevents them from penetrating into a solid zone. Because of using the same solution algorithm for both fluid and solid zones, it can be assumed that a similar effect on solid particles due to fluid flow would take place. In another words, fluid particles contribute only in the third step of the solution procedure of their solid neighbors.

It will be shown that the accuracy of presented the method is higher than the old one. It has other advantages such as: easier implementation, no special treatment for interface particles, less CPU time (it hasn't any extra procedure for interface calculation).

## 6. RIGID WALL BOUNDARY CONDITIONS

Boundary conditions always receive special attention in the SPH method; here the treatment used by Koshizuka et al. [26] was followed to model the wall boundaries by fixed wall particles, which are spaced according to the initial configuration. Here a kernel with a compact support of  $h = 1.5l_0$ , where  $l_0$  is the initial particle spacing, was employed. In addition, two lines of dummy particles with properties which are

completely similar to boundary particles are also placed outside of the solid walls at spacing  $l_0$ . The calculation procedure for both wall and dummy particles is completely similar to inner particles, except the zero velocity for no slip boundary conditions.

## 7. THE TEST CASE

In this section, a benchmark problem is studied to demonstrate the capability of the proposed method to solve fluid-structure interaction problems.

The benchmark problem is the deformation of an elastic plate subjected to time-dependent water pressure.

The results are compared with experimental data and results of the first attempt of SPH-FSI model [20] to show the better accuracy of the proposed algorithm.

Throughout this study and whatever the chosen smoothing length value, the typical distance (noted  $\Delta x$ ) between two particles is determined so that the interpolation circle contains about 20 particles (in a two dimensional context), that is,

$$\frac{h}{\Delta x} = 1.15 \quad (42)$$

It should be mentioned that the formulation utilized for elastic wall simulation is comparable with a fluid with large viscosity (with the order of  $G$ ), so the particles in the elastic solid zone have to be arranged closer to each other in comparison to fluid particles. In this simulation the initial spacing between solid particles is half of fluid ones, it means, the number of particles for showing the same amount of mass for an elastic solid zone is 2 times greater than a fluid one.

An elastic gate, clamped at one end and free at the other one, interacts with a mass of water initially confined in a free-surface tank behind the gate. A schematic view of this 2D problem is shown in Figure 1. As it is shown, the left wall consists in an upper rigid part and in a lower deformable plate made of rubber. The rubber plate is free at its lower end, thus representing an elastic gate closing the tank. The geometric dimensions of the system and the physical characteristics of the

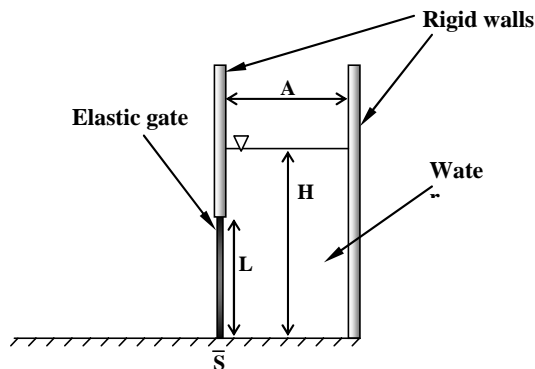


Figure 1. Schematic view of initial configuration.

elastic gate are reported in Table 1.

In Figure 2, the horizontal and vertical displacements computed for the plate (according to the presented SPH algorithm and FSI model) are compared with those measured in the digitalized images acquired during the experiments and the results of old SPH model of FSI.

Water level just behind the gate is shown in Figure 3. SPH particle positions at six different times are shown in Figure 4. These images are in complete agreement with the frames from the experiment setup at corresponding times (shown in [20]).

The evolution of the free-surface is also well reproduced by the simulation. Figure 4 shows the water level history immediately behind the gate.

As it can be seen, the accuracy of presented SPH simulation is completely greater than the old one. It is because of using a better algorithm for solid elastic simulation and no special treatment for interface particles (the interface modeled naturally).

## 8. CONCLUSION

This paper presents a numerical investigation of a fluid-structure interaction (FSI) model according to a modified Smoothed Particle Hydrodynamics (SPH) method.

The researchers have presented a new algorithm which models elastic-perfectly plastic solids using planar geometry, in the Lagrangian reference



TABLE 1. Dimensions of the System and Physical Characteristics of the Rubber Plate.

Dimensions	
A (m)	0.1
H (m)	0.14
L (m)	0.079
S (m)	0.005
Rubber	
$\rho$ (kg/m <sup>3</sup> )	1100
G (N/m <sup>2</sup> )	$4.27 \times 10^6$

frame. The modification of the utilized SPH concerns on removing the artificial viscosities and the artificial stresses (which such terms are commonly used to eliminate the effects of tensile and numerical instabilities). The new algorithm for elastic simulation is based on a prediction-correction procedure which has been used for fluid flow simulation. According to the presented method pressure Poisson equation (Equation 35) is utilized for pressure calculation instead of state equation which has some dependent constant to the materials and dynamics of the problems.

However, the purpose of this work was to propose a different method for Fluid-structure interaction modeling in engineering applications. It was shown that this method has some advantages

such as more accuracy and easier programming compared to other methods in similar cases. The mentioned performance of the proposed algorithm is assessed by solving a test case including deformation of an elastic plate subjected to time-dependent water pressure. The obtained results are in close agreement with other high accuracy methods and experimental results.

## 9. NOMENCLATURE

A A Typical Field Variable  
 r Position Vector

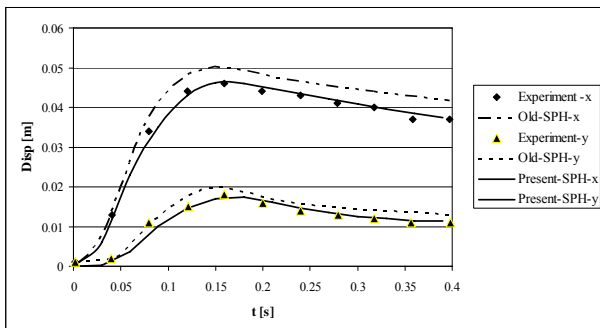


Figure 2. Horizontal and vertical displacements of the free end of the plate.

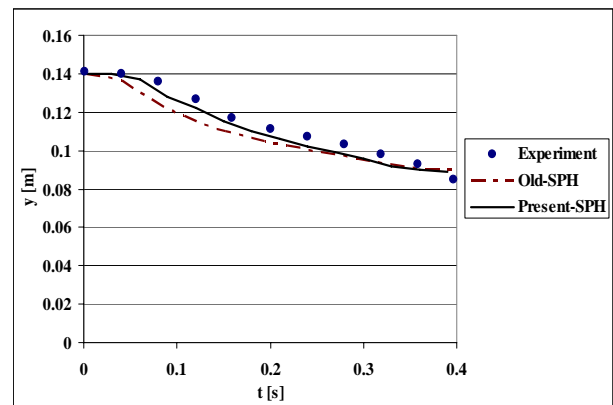
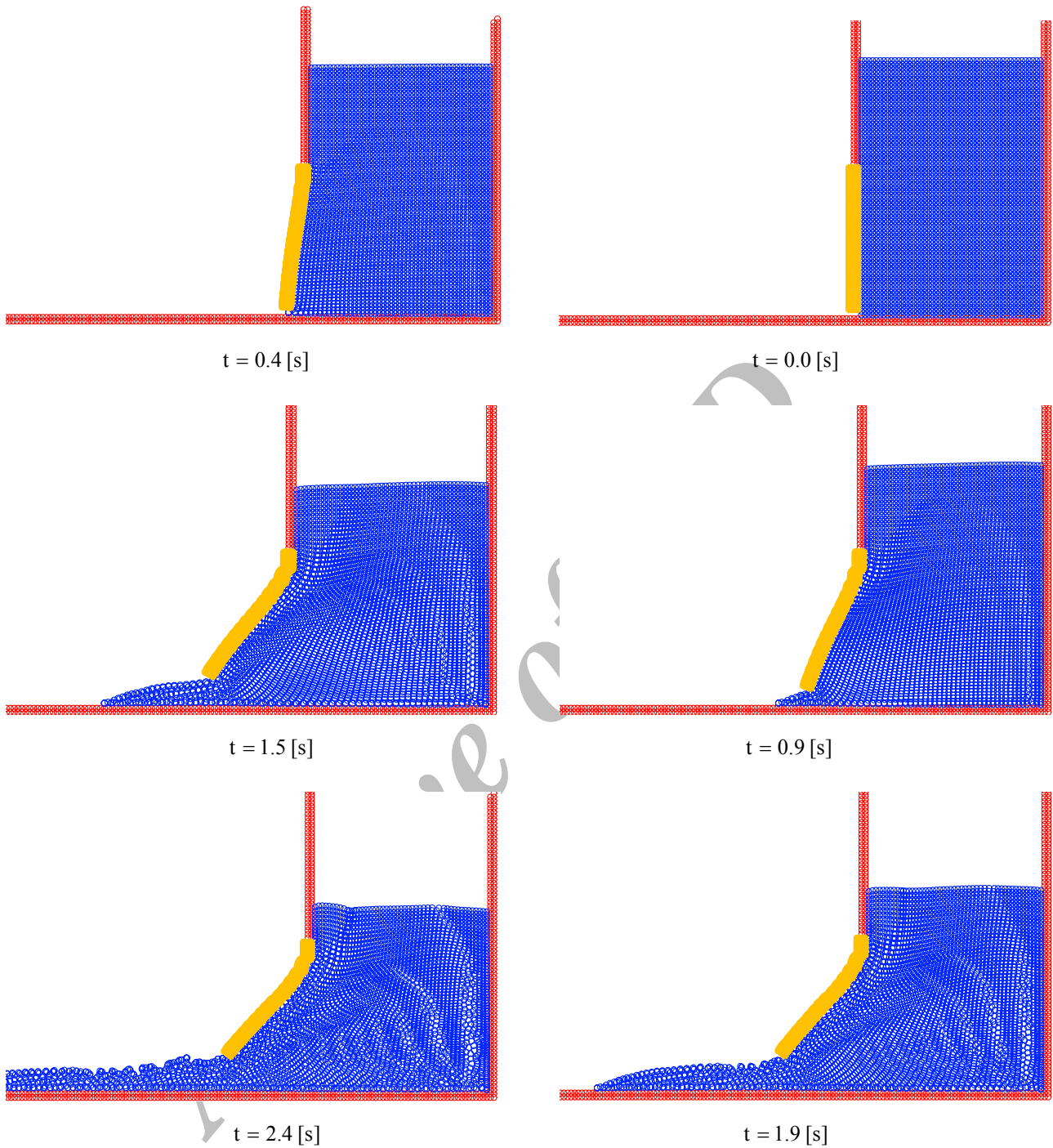


Figure 3. Water level (m) just behind the gate.



**Figure 4.** SPH particle positions at six different times.

W Weight Function (Kernel)  
h Smoothing Length  
V Volume

$\delta$  Dirac Delta Function  
 $\sigma$  Normalized Constant  
 $u$  Number of Dimensions

m	Mass of Particle
$\rho$	Density
v	Velocity
s	Normalized Position Variable
u	Velocity Vector
V	Velocity Vector
$\tau$	Viscous Stress Tensor
g	Gravity Force Per Unit Mass
S	Shear Strain
P	Pressure
t	Time
$\Delta x$	Space Step

### Subscripts

i	Target Particle Index
j	Neighborhood Particle Index
Y	Yeilding Point
x	Normal in x-Direction
y	Normal in y-Direction
xy	Shear Direction in x-y Plain.
0	Reference Values
t	Time Index
$\Delta t$	Time Step

### Superscripts

*,**	Temporal Variables
^	Field Variables
.	Time Derivity

## 10. REFERENCES

- Jaroslav Hron, Martin Mádlik, Fluid-structure interaction with applications in biomechanics, *Nonlinear Analysis: Real World Applications*, Article In Press, (2006), 1431-1458.
- Van Loon, R., Anderson, P. D. and Van De Vosse, F. N. "A fluid-structure interaction method with solid-rigid contact for heart valve dynamics", *Journal of Computational Physics*, Vol. 217, (2006), 806-823.
- Hirt, C. W., Amsden, A. A. and Cook, J. L. "An arbitrary Lagrangian-Eulerian computing method for all speeds", *J. Comput. Phys.*, Vol. 14, (1974), 227-253.
- Donea, J., Giuliani, S. and Halleux, J. P., "An arbitrary Lagrangian-Eulerian finite element method for transient dynamic fluid-structure interactions", *Comput. Meth. Appl. Mech. Eng.*, Vol. 33, (1982), 689-723.
- Peskin, C. S., "The immersed boundary method", *Act. Num.*, Vol. 11, (2002), 479-517.
- Glowinski, R., Pan, T. W. and Pe'riaux, J., "A Lagrange multiplier/fictitious domain method for the numerical simulation of incompressible viscous flow around moving rigid bodies", *C. R. Acad. Sci. Paris*, Vol. 25, No. 5, (1997), 361-369.
- Glowinski, R., Pan, T. W., Hesla, T. I. and Joseph, D. D., "A distributed Lagrange multiplier/fictitious domain method for particulate flows", *Int. J. Multiphase Flow*, Vol. 324, (1999), 755-794.
- Baaijens, F. P. T., "A fictitious domain/mortar element method for fluid-structure interaction", *Int. J. Num. Meth. Fluids*, Vol. 35, No. 7, (2001), 743-761.
- Dai, F. and Rajagopal, K. R. "Diffusion of fluids through transversely isotropic solids", *Acta Mech.*, Vol. 82, (1990), 61-98.
- Spilker, R. L., Suh, J. K. and Mow, V. C., "Finite element formulation of the nonlinear biphasic model for articular cartilage and hydrated soft tissues including strain-dependent permeability", *Comput. Meth. Bioeng.*, Vol. 9, (1988), 81-92.
- Lucy, L. B., "A numerical approach to the testing of the fission hypothesis Astron", *J. of Astronomy*, Vol. 82, 1013-24
- Gingold, R. A. and Monaghan, J. J., "Smoothed particle hydrodynamics theory and application to non-spherical stars", *Mon. Not. R. Astronom. Soc.*, Vol. 181, (1977), 375.
- Monaghan, J. J., "Simulating free surface flows with SPH", *J. Comp. Physics*, Vol. 110, (1994), 399.
- Chaniotis, A. K., Poulidakos, D. and Koumoutasakos, P., "Remeshed smoothed particle hydrodynamics for the simulation of viscous and heat conducting flows", *J. Comp. Physics*, Vol. 182, (2002), 67-90.
- Owen, J. M., "Remeshed smoothed particle hydrodynamics for the simulation of viscous and heat conducting flows", *J. Comp. Physics*, Vol. 182, (2002), 67-90.
- Takeda, H., Miyama, S. M. and Sekiya, M., "Numerical Simulation of Viscous Flow by Smoothed Particle Hydrodynamics", *Progress of Theoretical Physics*, Vol. 92, No. 5, (1994), 939-960.
- Cleary, P., Ha, J., Alguine, V. and Nguyen, T., "Flow modelling in casting processes", *Applied Mathematical Modelling*, Vol. 26, (2002), 171-190.
- Oger, G., Doring, M., Alessandrini, B. and Ferrant, P., "Two-dimensional SPH simulations of wedge water entries", *J. Comp. Physics*, (2005), 803-822.
- Gray, J. P., Monaghan, J. J. and Swift, R. P., "SPH elastic dynamics", *Comp. Methods Appl. Mech. Eng.*, Vol. 190, (2001), 6641-6662.
- Antoci, C., Gallati, M. and Sibilla, S., "Numerical simulation of fluid-structure interaction by SPH", *Computers and Structures*, (2007), 879-890.
- Monaghan, J. J., "Smoothed particle hydrodynamics", *Annul. Rev. Astron. Astrophys.*, Vol. 30, (1992), 543-574.
- Colagrossi, A. and Landrini, M., "Numerical simulation of interfacial flows by smoothed particle hydrodynamics", *J. Comp. Phys.*, Vol. 191, (2003), 448-475.
- Cummins, S. J. and Rudman, M., "An SPH projection method", *J. Comp. Phys.*, Vol. 152, (1999), 584-607.

24. Howell, B. P. and Bally, G. J., "A Free-Lagrange Augmented Godunov Method for the Simulation of Elastic-Plastic Solids", *J. Comp. Phys.*, Vol. 175, (2002), 128-167.
25. Randles, P. W. and Libersky, L. D., "Smoothed particle hydrodynamics: some recent improvements and applications", *Comput Methods Appl Mech Eng*, Vol. 139, (1996), 375-408.
26. Koshizuka, S., Oka, Y. and Tamako, H., "A particle method for calculating splashing of incompressible viscous fluid", *Internation Conference on Mathematics and Computations*, Vol. 2, (1995), 1514-1526.
27. Edmond, S. S. and Lo, Y. M., "Incompressible SPH method for simulating Newtonian and non-Newtonian flows with a free surface", *Advances in Water Resources*, Vol. 26, (2003), 787-800.
28. Hosseini, S. M., Manzari, M. T. and Hannani, S. K., "A fully explicit three step SPH algorithm for simulation of non-Newtonian fluid flow", *Int. J. of Numerical Methods for Heat and Fluid Flow*, Vol. 1, No. 1, (2007), 1-10.

Archive of SID